Silver Inkjet-Printed Electrode on Paper for Electrochemical Sensing of Paraquat

Patricia Batista Deroco [ID], Dagwin Wachholz Junior [ID] and Lauro Tatsuo Kubota *

Institute of Chemistry, University of Campinas—UNICAMP, 13083-970 Campinas, Brazil;
patyderoco@hotmail.com (P.B.D.); dagwinjr@gmail.com (D.W.J.)
* Correspondence: kubota@unicamp.com; Tel.: +55-19-3521-3127

Abstract: The use of fully printed electrochemical devices has gained more attention for the monitoring of clinical, food, and environmental analytes due to their low cost, great reproducibility, and versatility characteristics, serving as an important technology for commercial application. Therefore, a paper-based inkjet-printed electrochemical system is proposed as a cost-effective analytical detection tool for paraquat. Chromatographic paper was used as the printing substrate due its sustainable and disposable characteristics, and an inkjet-printing system deposited the conductive silver ink with no further modification on the paper surface, providing a three-electrode system. The printed electrodes were characterized with scanning electron microscopy, cyclic voltammetry, and chronopotentiometry. The proposed sensor exhibited a large surface area, providing a powerful tool for paraquat detection due to its higher analytical signal. For the detection of paraquat, square-wave voltammetry was used, and the results showed a linear response range of 3.0–100 μM and a detection limit of 0.80 μM, along with the high repeatability and disposability of the sensor. The prepared sensors were also sufficiently selective against interference, and high accuracy (recovery range = 96.7–113%) was obtained when applied to samples (water, human serum, and orange juice), showing the promising applicability of fully printed electrodes for electrochemical monitoring.

Keywords: printed electronics; electroanalysis; disposable electrode; chromatographic paper; paraquat determination; silver ink; inkjet printing

1. Introduction

The development of fully printed analytical devices has been increasingly active in the market of printed electronics. It is estimated that, in 2020, the market reached around $7.8 billion, and it is expected to increase to $20.7 billion by 2025 [1]. This growth is due to the use of analytical devices for real-time detection in clinical, food, and environmental applications, which are crucial technologies for improving well-being and life quality. Especially in low- and middle-income countries, many people suffer unnecessarily due to the lack of access to these technologies at affordable prices. Printed electrochemical sensors represent an important cost-effective analytical detection technology for disposable and one-shot use sensors, which are a powerful and extremely necessary tool to fill this gap [2]. Moreover, the ability to achieve highly sensitive analytical detection without the requirement of further modification to printed electrochemical sensors gives them high potential for industrial production and commercialization, where minimal costs and ease of production are essential [3].

With the evolution of microelectronics and the possibility of automatization, electrochemical sensors have become more available, demonstrating reliable performance for the detection of important analytes and applicability in the real world. Thus, the development of disposable printed electrodes is gaining importance globally, and many notable works have been reported in the literature [4–6]. In the search for low-cost devices, the application of paper as a substrate for printed electrodes has attracted great attention recently due to

the abundance of the material, and they are a more sustainable and disposable alternative to conventional materials, such as glass or polymers [7–9]. Additionally, interesting designs of devices with paper substrates can be realized to allow the simultaneous measurement (detection) of several analytes from a single sample with the combination of different detection techniques. Due to its versatility, paper allows the construction of innovative devices with the integration of several analytical procedures, such as reagent pre-location, chromatographic separations, pre-concentration steps, integration of sample pre-treatment systems, and so on [10,11].

Among the various techniques for the deposition of conductive materials on paper, screen- and inkjet-printing technologies are the most attractive because these processes are versatile, low-cost, and suitable for miniaturization and large-scale production [9,12]. Particularly, inkjet printing is a deposition technology that digitally controls small ejected drops (in the picoliter–nanoliter range) of ink in specific locations on the substrate in a fully automated manner, which allows high precision and resolution with great reproducibility of the printed electrodes [13]. Moreover, the great advantage of inkjet printing over screen printing is that no mask is required. Specific patterns, according to users' needs, can be projected on the computer using common graphic drawing software and sent directly to the printer [14,15]. Although commercial ink formulations are available, there are also countless possibilities for the development of conductive inks containing functional materials, such as biomolecules and nanomaterials [16–18].

Despite their advantages, there are still few reports of the use of the inkjet-printing technique to manufacture electrochemical sensors when compared to those using the screen-printing technique. For these reasons, we report the development of a fully printed electrochemical device based on chromatographic paper using an inkjet-printing technique with conductive silver ink and without further modification in order to explore the suitability of the material and technique for use in electrochemical detection.

In this work, the pesticide paraquat was chosen as a representative molecule for performance evaluation of the printed electrode. Paraquat is one of the most toxic substances and widely used in agriculture in more than 100 countries [19]. Although it is only slightly adsorbed by the soil, paraquat is a potential contaminant of water due to its high solubility, becoming potentially dangerous for aquatic systems and consequently for human and animal health [20]. Since paraquat is considered a non-polluting herbicide, it is often used indiscriminately, increasing its toxicological potential and the risk posed to human health. Consequently, many studies have demonstrated the detection of paraquat using different electrodes, such as modified glassy carbon electrodes [21–26], hanging mercury drop electrodes [27], and screen-printed electrodes [28,29]. These reported devices, however, suffer from high material and manufacturing costs, have poor disposability, are not suitable for portable detection, and involve complex electrode modification steps in some cases.

Therefore, the purpose of using a paper-based silver electrode deposited by the inkjet-printing method is to meet requirements for high performance, low-cost, and disposability; eliminate the so-called memory effect caused by surface contamination; and provide an efficient tool for the simple and cost-effective monitoring of intended analytes.

2. Materials and Methods

2.1. Reagents and Standards

The standards of paraquat dichloride (methyl viologen), potassium ferricyanide $K_3[Fe(CN)_6]$, and hexaammineruthenium(III) chloride $[Ru(NH_3)_6]Cl_3$ were purchased from Sigma-Aldrich, while Na_2SO_4 was purchased from Merck and used without further purification. All other reagents were of analytical grade, and all solutions were prepared in ultrapure water ($\rho \geq 18.2$ MΩcm) obtained using a Milli-Q system. A 0.01 mol L^{-1} stock solution of paraquat was prepared daily in a 0.1 mol L^{-1} Na_2SO_4 aqueous solution, which was also used as the supporting electrolyte.

Silver nanoparticle (AgNP) ink for the inkjet printer (<50 nm, 20 wt.% in ethylene glycol) and the substrate Whatman#1® chromatographic paper were also purchased from

Sigma-Aldrich. A commercial bleach solution (approximately 40 mg mL^{-1} NaClO) was used to modify the silver surface to obtain a pseudo-reference electrode (Ag/AgCl).

A sample of orange fruit was purchased from a local supermarket. First, the juice of five oranges was manually extracted, homogenized, and centrifugated, and the supernatant was used for the analysis. Tap water samples were collected at the University of Campinas (São Paulo, Brazil) and used without any treatment. Human serum (male, AB, filtered, and sterile) was purchased from Sigma-Aldrich (St. Louis, MO, USA) and centrifugated, and the supernatant was used for the analyses.

Before the analyses, all samples were spiked with paraquat. Then, aliquots of 200 µg/L of each sample were diluted in the supporting electrolyte solution, and final solutions with a concentration of 30 µmol L^{-1} paraquat were analyzed.

2.2. Apparatus

A piezoelectric Dimatix Materials Printer DMP-2831, FUJIFILM Dimatix, Inc., Santa Clara, CA, USA, was used to print the AgNP ink on the paper substrate.

The electrochemical measurements were performed using an AUTOLAB PGSTAT-30 potentiostat/galvanostat (Metrohm/Eco Chemie, Utrecht, The Netherlands) interfaced with a computer and managed by NOVA 2.1 software (Metrohm/Eco Chemie, Utrecht, The Netherlands).

To evaluate the performance of the proposed inkjet-printed pseudo-reference electrode, a two-electrode system was used with a commercial Ag/AgCl (saturated KCl solution) reference electrode (Methrom/Eco Chemie, Utrecht, Netherlands). A conventional three-electrode system was also used, including a Pt wire as the auxiliary electrode, glassy carbon as the working electrode, and the proposed pseudo-reference electrode.

A field-emission scanning electron microscope (SEM), model JEOL J6360 LV (JEOL Ltd., Tokyo, Japan) operating at a voltage of 20 kV, was used to morphologically characterize the silver film on paper.

An Eppendorf centrifuge (model 5418 R) (Eppendorf Zentrifugen GmbH, Leipzig, Germany) with a speed capacity of 100–14,000 rpm was used to centrifuge the samples.

An optical microscope (AmScope B120C) equipped with a Fixed Microscope Adapter (FMA050) (AmScope, Irvine, CA, USA) was used to obtain images and determine the geometrical area of the printed electrode. The images were processed with Adobe Photoshop® CC 2019 Software, Adobe, San Jose, CA, USA, in order to normalize the areas, considering a standard pattern in the same amplification of the microscope. The areas of 15 different electrodes were determined to get the average value and evaluate the repeatability.

2.3. Paper-Based Inkjet Sensor Printing

First, 1.5 mL of the AgNP ink was injected into a 10 pL DMC-116110 cartridge. Then, a three-electrode system was designed using CorelDraw® software, Corel, Ottawa, Canada and printed on chromatographic paper using the inkjet Dimatix Printer, FUJIFILM Dimatix, Inc., Santa Clara, CA, USA. The waveform used to print was "Dimatix Model Fluid 2 Waveform" with a voltage between 16 and 20 V. The printing process was carried out at room temperature, and cleaning cycles (Purge 1.0 s Blot) were used only before printing. A spacing of 30 µm between two consecutive drops and 4 layers of ink were necessary to obtain a conductive silver film on chromatographic paper. After each layer, the silver ink was cured at 120 °C for 20 min.

Next, a specific hydrophobic pattern barrier was printed on paper using a ColorQube 8570 office printer from Xeroxand employing cartridge-free ColorQube solid ink—Xerox 108R00940 (Xerox Corporation Norwalk, CT, USA). The wax-printed sheet was kept in an oven for 1 min at 100 °C in order to melt the wax and create a hydrophobic wall due to its penetration into the porous paper.

The geometric area of the working electrode was determined using microscope images, and a value of 0.080 ± 0.001 cm^2 (n = 15, RSD = 1.61%) was obtained. This new sensor was referred to as the paper-based silver sensor.

The pseudo-reference electrode was prepared using a procedure developed by Silva et al. [30]. The Ag/AgCl formation was carried out by depositing a drop of bleach solution just on top of the pseudo-reference electrode for 30 s, which was then rinsed with ultra-pure water. The obtained pseudo-reference electrode was then used without any further modification.

2.4. Electrochemical Measurements

Chronopotentiometric measurements were employed to characterize the electrochemical activity of the Ag/AgCl pseudo-reference electrode against a commercial Ag/AgCl reference electrode. These measurements of open circuit potential were carried out in saturated KCl solution for 15 min.

The paraquat electrochemical behavior was investigated using cyclic voltammetry (CV), whereas the determination of this analyte was performed using square-wave voltammetry (SWV). The SWV conditions used were f = 3 Hz; a = 60 mV; ΔE = 2 mV.

All measurements were performed in triplicate (n = 3) using three different disposable electrodes by simply dropping 50 µL of the sample on the sensor testing area.

The limits of detection (LOD) and quantification (LOQ) were calculated using the equation 3 (Sy/b) and 10 (Sy/b), respectively, where Sy is the standard deviation of the intercept and b the slope of the analytical curve [31].

3. Results

3.1. Morphological and Electrochemical Characterization of Inkjet-Printed Sensors

First, the effect of the number of printed silver nanoparticles layers on the paper substrate was investigated to optimize the conductivity of the inkjet-printed electrode. After each printing step, the resistance of the printed layer was measured in order to achieve the lowest value. It was observed that the resistance of the printed electrode decreased, and the current signal for the silver cyclic voltammetric profile was enhanced as the number of printed layers increased (Figure S1). After four layers of silver ink deposition, a constant and lower resistance value and high current signal were achieved. Therefore, this condition was chosen for the printing step of the electrode.

The images obtained from scanning electron microscopy (SEM) before (Figure 1A) and after the printing of silver ink (Figure 1B,C) show that with the inkjet-printing process, the paper fibers were clearly modified and totally surrounded by silver nanoparticles of approximately 50 nm (Figure 1C). The SEM and optical images (Figure 1D) also show the high porosity of the paper substrate, indicating a large surface area of the electrode. The roughness of the electrode border seen in Figure 1D can be attributed to the porosity of the paper, which allows the silver ink to percolate into the pores of the substrate, which may increase the electroactive area of the electrode.

The performance of the inkjet-printed solid-state Ag/AgCl pseudo-reference electrode was evaluated by chronopotentiometry in saturated KCl against a commercial Ag/AgCl (saturated KCl solution) reference electrode (Figure 2A). As can be observed, there is no significant difference between these electrodes (open circuit potential value measured of 0.3 ± 0.1 mV), which highlights the stability of the proposed pseudo-reference electrode. As reported by Silva et al. [30], this small deviation from the ideal value of zero may be attributed to slight differences in the chloride activity in the test solution and the commercial reference filling solution or to an uncertain junction potential. The reliability of the proposed pseudo-reference was also confirmed by cyclic voltammograms obtained for the glassy carbon electrode using the pseudo-reference electrode (duplicate) or commercial Ag/AgCl in the presence of 1.0 mmol L^{-1} $K_3[Fe(CN)_6]$ in 0.1 mol L^{-1} KCl solution at v = 50 mV s^{-1}. As can be observed in the inset of Figure 2A, the potential value did not change in the cyclic voltammograms using a different reference electrode, demonstrating the high stability of the proposed pseudo-reference electrode in maintaining a constant potential.
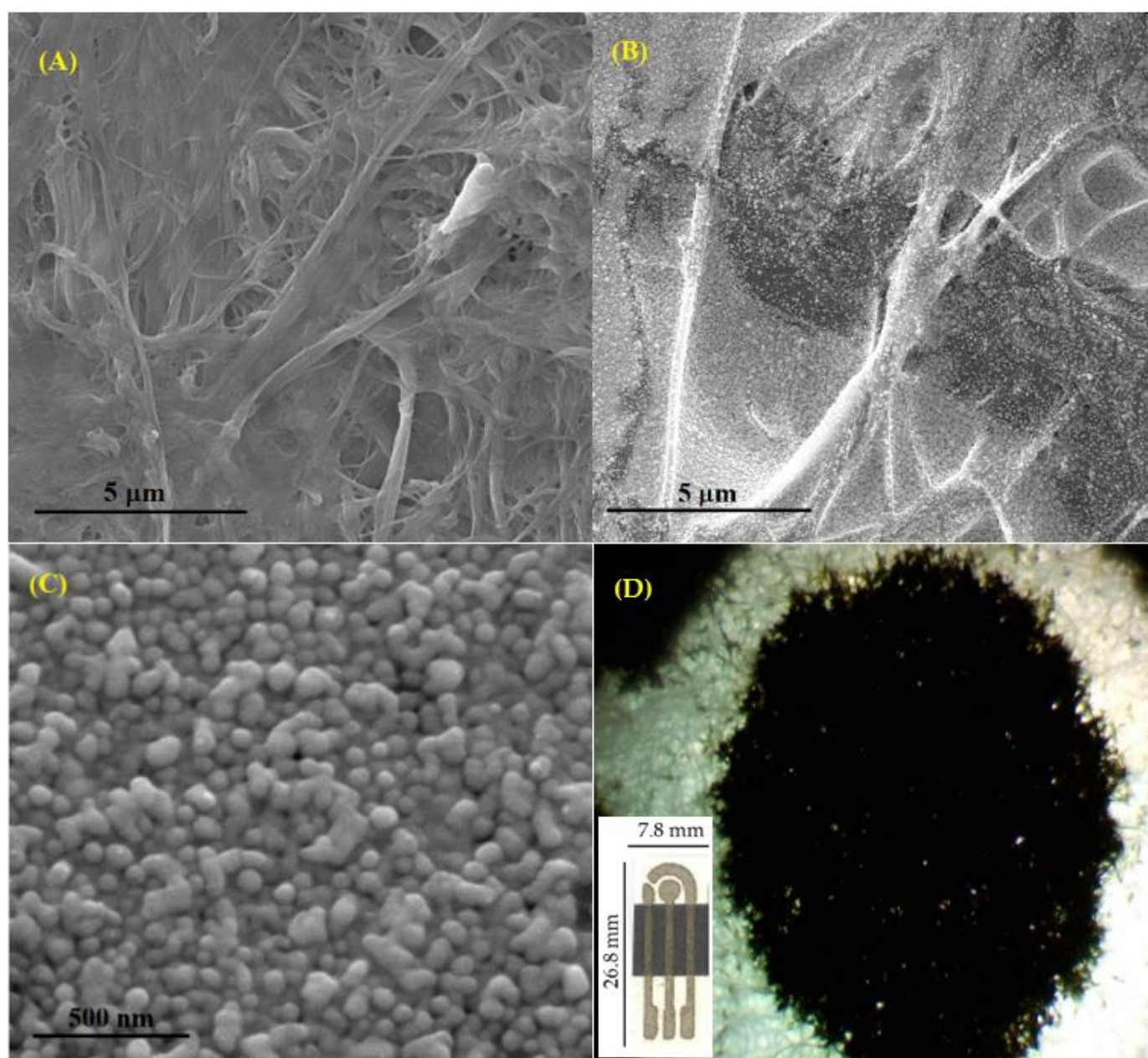
Figure 1. SEM images obtained from the (**A**) bare paper and (**B**,**C**) silver electrode surface printed on the paper substrate at different magnifications. Optical image (**D**) of the silver electrode. The inset is the photo of the three-electrode system.

The effectiveness of the paper-based silver three-electrode system (inset in Figure 1B) was evaluated using the CV technique and a $[Ru(NH_3)_6]Cl_3$ electrochemical probe. Figure 2B shows the cyclic voltammograms obtained by varying the potential scanning rate (10–500 mV s^{-1}) for a solution of 1.0 mmol L^{-1} $[Ru(NH_3)_6]Cl_3$ in 0.1 mol L^{-1} phosphate buffer pH 7.0, as well as the currents of the anodic peak (I_{pa}) and cathodic peak (I_{pc}) plots as a function of the square root of the scan rate (inset). It can be observed that both (I_{pa} and I_{pc}) vary linearly with the square root of the scan rate, indicating that the process was fully controlled by the diffusion of the electroactive species. The diffusion of the species was also confirmed by the log I vs. log v plot, which presented an angular coefficient of 0.6. This value is close of the theoretical reported value of 0.5 for diffusion-controlled processes [32]. From the results obtained in this study, the electroactive area for the proposed sensors was calculated by employing the Randles–Sevcik equation [33]. For $[Ru(NH_3)_6]Cl_3$, D = 9.78 × 10^{-6} cm^2 s^{-1} [34], n = 1, and C = 1.0 × 10^{-6} mol cm^{-3}, the obtained elec-

troactive area value (1.58 cm^2) was almost 20 times bigger than the geometric area of 0.080 ± 0.001 cm^2. This response suggests that the silver electrode surface is highly porous, in agreement with SEM images (Figure 1). This property results in a higher analytical signal, demonstrating the potential of this electrode for analytical applications.
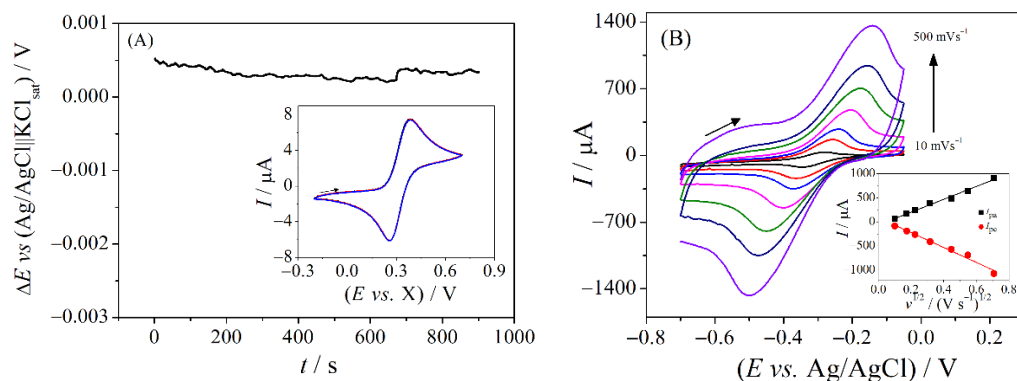

Figure 2. (**A**) Chronopotentiometric analysis comparing the behavior of the Ag/AgCl pseudo-reference electrode inkjet-printed on paper against a commercial Ag/AgCl (saturated KCl solution). The insets are cyclic voltammograms obtained using a glassy carbon electrode and the pseudo-reference electrode (duplicate) or commercial Ag/AgCl in the presence of 1.0 mmol L^{-1} K$_3$[Fe(CN)$_6$] in 0.1 mol L^{-1} KCl solution. (**B**) Cyclic voltammograms obtained using the paper-based silver sensor at different potential scanning rates (10–500 mVs^{-1}) in the presence of 1.0 mmol L^{-1} [Ru(NH$_3$)$_6$]Cl$_3$ in 0.1 mol L^{-1} phosphate buffer pH 7.0. The inset graph shows the linear relationship of the anodic and cathodic peak currents as a function of the square root of the potential scan rate.

The heterogeneous electron transfer constant (k^0) was also estimated from the same cyclic voltammetry data at different scan rates by applying the Nicholson method (for quasi-reversible systems controlled by diffusion) [35]. In this method, the value of k^0 is obtained using following equation:

$$\psi = k^0 \left[\frac{\pi D n v F}{RT} \right]^{-1/2}$$

where ψ is the kinetic parameter, $D = 9.78 \times 10^{-6}$ cm^2 s^{-1}, $n = 1$, F is the Faraday's constant (96,485 C mol^{-1}), $R = 8.314$ J K^{-1} mol^{-1}, and $T = 298.15$ K. The ψ values were calculated from the ΔE_p values verified at each scan rate using an empirical equation proposed by Lavagnini et al. [36]:

$$\psi = \frac{(-0.6288 + 0.0021 n \Delta E p)}{(1 - 0.017 n \Delta E p)}$$

From the calculated ψ values, the k^0 value for the [Ru(NH$_3$)$_6$]Cl$_3$ redox reaction was determined to be 0.0040 cm s^{-1}. The value is better than or comparable to the same parameter obtained using a paper graphitic SPE electrode (0.0012 cm s^{-1}) [37] and (0.00072 cm s^{-1}) [38] and a platinum nanoparticle-decorated vertically aligned graphene SPE electrode (0.0041 cm s^{-1}) [39].

3.2. Electrochemical Behavior of Paraquat Pesticide

Cyclic voltammograms of samples with and without paraquat were recorded in 0.1 mol L^{-1} Na$_2$SO$_4$ solution (pH 7.0) to evaluate its electrochemical behavior using the developed sensor. The Na$_2$SO$_4$ solution was chosen as the supporting electrolyte because it has previously led to good responses for this analyte, as demonstrated in other works [21,40–42].

As shown in Figure 3, in the absence of paraquat (black dashed line voltammogram), no faradaic process was observed, corresponding to the response of the bare electrode related to the intrinsic structure and surface of the sensor; when adding paraquat, two

quasi-reversible cathodic peaks at -0.38 V and at -0.86 V and two overlapping (as seen by the peak distortion) anodic peaks around -0.68 V (vs. Ag/AgCl) were observed. According to the literature data, the first one is related to the reversible electrochemical reduction involving the formation of the radical $PQ^{\bullet+}$ cation (Equation (1)), while the second one is related to the reduction of this generated species, forming the neutral molecule PQ^0 (Equation (2)) [28,43]. Coproportionation can also occur between PQ^0 and PQ^{2+} to generate two $PQ^{\bullet+}$. The reduction scheme may be represented by the following equations:

$$(1)$$

$$(2)$$
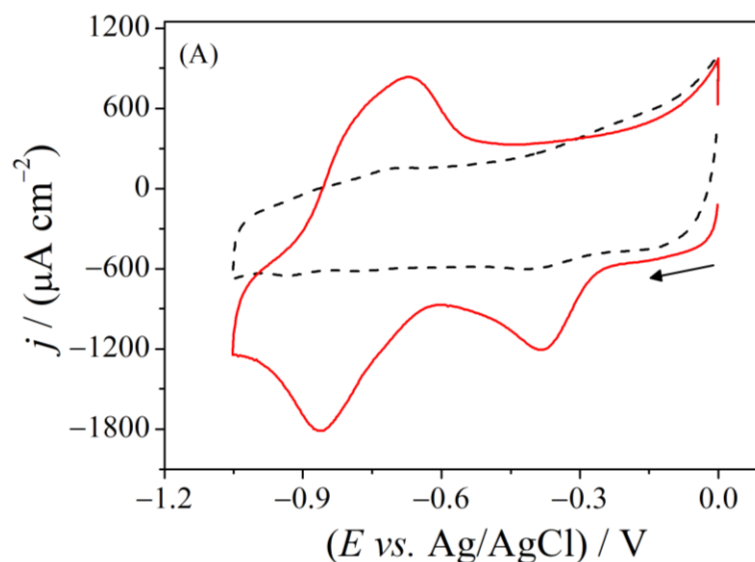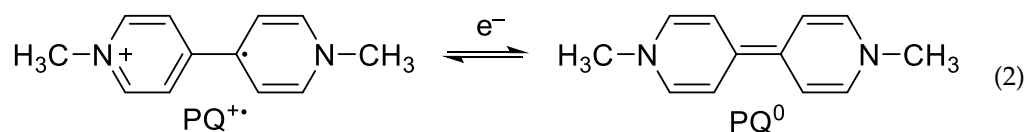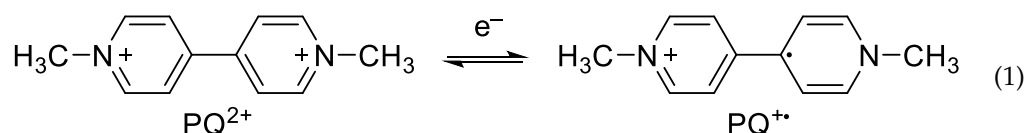
Figure 3. Cyclic voltammograms obtained using a paper-based silver sensor in the absence (black dashed line) and in the presence (red solid line) of 1.0 mmol L^{-1} paraquat in 0.1 mol L^{-1} Na_2SO_4, $v = 100$ mV s^{-1}.

The oxidation process at -0.68 V was used for further study because, at this potential, higher detectability was achieved in comparison to that obtained in the two cathodic processes.

3.3. Determination of Paraquat Using SWV

Preliminary studies on the effect of SWV parameters on the redox process of paraquat were evaluated in the conditions presented in Table 1. The best electrochemical response was selected from the obtained voltammograms with low background noise and a well-defined and high-intensity peak for paraquat, as can be inferred from the data in Figures S1–S3 in Supplementary Materials.

Table 1. Optimization of experimental conditions for paraquat detection using the square-wave voltammetry (SWV) technique.

Parameter	Evaluated Conditions	Best Conditions
SWV frequency (f)	3–10 Hz	3 Hz
SWV amplitude (a)	10–70 mV	60 mV
SWV potential increment (ΔE)	1–5 mV	2 mV

Next, square-wave voltammograms were registered under optimized conditions for varied concentrations of paraquat in 0.1 mol L^{-1} Na$_2$SO$_4$ in order to build the analytical curve. The obtained graphs are presented in Figure 4. The analytical curve for paraquat (Figure 4B) is linear in the range from 3.0 to 100 μmol L^{-1}, with a linear correlation equal to I (A) = $-3.588 \times 10^{-7} + 6.176 \times 10^{-7}$ (A L μmol^{-1}) C_{paraquat} (r = 0.999). The LOD and LOQ values (calculated as described in the experimental procedure) were 0.80 μmol L^{-1} and 2.5 μmol L^{-1}, respectively. Although the achieved LOD is not the best in comparison with those reported in previous studies (Table 2), it is better than some [44,45], and compared with others [23,46], it is clearly acceptable. It is also worth mentioning that while some sensors showed lower detection limits, their linear range was narrower than that of the proposed sensor. The printed sensor also has the great advantage of being produced without further modification steps when compared to all other chemically modified electrodes and is a potential platform for sustainable and disposable monitoring devices.
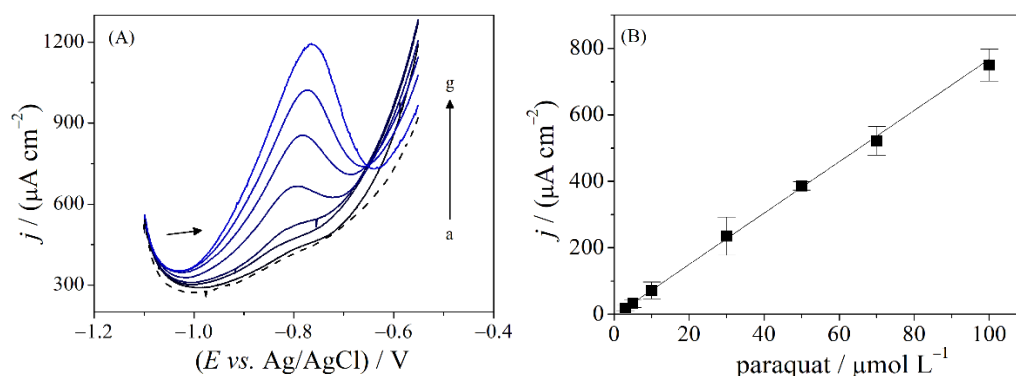

Figure 4. (**A**) Square-wave voltammograms obtained using the paper-based silver sensor in the absence (dashed line) and presence of different concentrations of paraquat (solid line: (a) 3.0 μmol L^{-1}, (b) 5.0 μmol L^{-1}, (c) 10.0 μmol L^{-1}, (d) 30.0 μmol L^{-1}, (e) 50.0 μmol L^{-1}, (f) 70.0 μmol L^{-1}, and (g) 100 μmol L^{-1})) in 0.1 mol L^{-1} Na$_2$SO$_4$ solution. (**B**) The respective analytical curve. SWV conditions: f = 3 Hz; a = 60 mV; ΔE = 2 mV.

3.4. Repeatability, Selectivity, and Sample Analysis

To assess the fabrication repeatability of the proposed sensor, inter-electrode measurements were performed on the same day with five different sensors (n = 5). This study was carried out for two concentration of paraquat (10.0 μmol L^{-1} and 70.0 μmol L^{-1}) in a 0.1 mol L^{-1} Na$_2$SO$_4$ solution, as seen in Figure 5. The relative standard deviation (RSD) values obtained were 7.1% and 4.1%, respectively, indicating the high repeatability of the sensor fabrication method. This behavior is due to the simplicity and automatization of the procedure adopted for the fabrication of electrochemical sensors.

Table 2. Comparison of the performance of different chemically modified electrodes for the detection of paraquat (PQ).

Electrode	Linear Range (μmol L^{-1})	LOD (μmol L^{-1})	Technique	Reference
CB-alginate film/GCE	1.6–7.8	0.23	SWV	[23]
AgNP/MWCNT/Nafion/GCE	0.10–10	0.07	AsDPV	[24]
BN/MoS$_2$/AuNPs/GCE	0.10–100	0.07	DPV	[25]
HMDE	0.25–1.7	0.04	DPCSV	[27]
Bi/SPM	0.12–4.2	0.01	DPV	[28]
CNT-Nafion/SPE	0.54–4.3	0.02	SI-DPV	[29]
AuNPs/DNA/GCE	5.0–3000	1.3	DPV	[44]
GCE	3.9–31.0	3.2	SWV	[45]
Cu$_2$O/PVP-GNs/GC-RDE	1.0–200	0.26	DPV	[46]
Paper-based silver sensor	3.0–100	0.80	SWV	This work

CB = carbon black; GCE = glassy carbon electrode; AgNP = silver nanoparticles; MWCNT = multiwall carbon nanotubes; AsDPVs = adsorptive differential pulse voltammetry; BN = boron nitride; AuNPs = gold nanoparticles; HMDE = hanging mercury drop electrode; DPCSV = differential pulse cathodic stripping voltammetry; Bi/SPM = bismuth film screen-printed mini sensor; CNT = carbon nanotubes; SPE = screen-printed electrode; SI-DPV = sequential injection differential pulse voltammetry; PVP-GNs: polyvinyl pyrrolidone functionalized graphene nanosheets; GC-RDE: glassy carbon-rotating disk electrode.
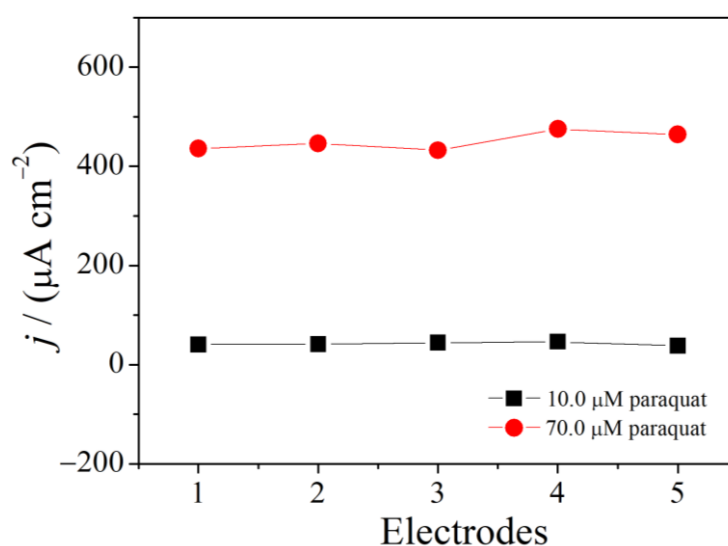
Figure 5. Analytical signal obtained in the inter-electrode repeatability study for the determination of paraquat (at two different concentrations) in 0.1 mol L^{-1} Na$_2$SO$_4$ solution using SWV and the proposed paper-based silver sensor.

The selectivity of the printed sensor was evaluated in an interference study (Figure 6), where a 50.0 μmol L^{-1} paraquat solution was analyzed in the absence and in the presence of different chemical species (glucose, albumin, ascorbic acid, and different metal cations) that were considered as possible interferents at a concentration ratio of 1/10 (analyte/interferent). The measurements were made in triplicate (n = 3), and the error bars correspond to the relative standard deviation between them.
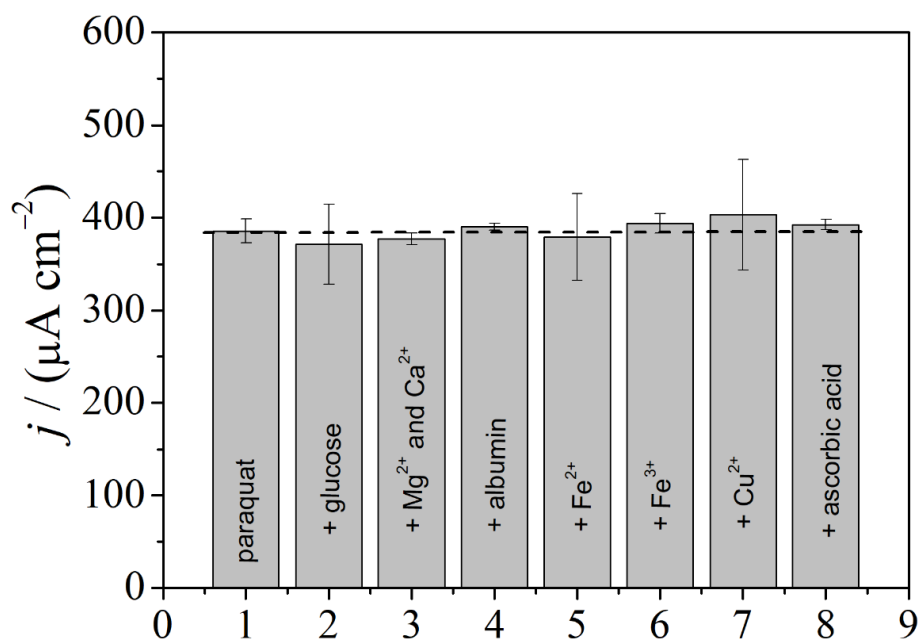
Figure 6. Effect of possible interferents on the SWV determination of a 50.0 μmol L^{-1} paraquat solution at 1/10 concentration ratios (analyte/interferent) in 0.1 mol L^{-1} Na$_2$SO$_4$ solution using the paper-based silver sensor.

As shown in Figure 6, the signals recorded with the addition of interfering species remained practically constant in comparison with the paraquat oxidation signal obtained in the absence of these investigated interferents (the voltammograms obtained can be seen in Figure S5 in Supplementary Materials). Thus, it is possible to conclude that paraquat can be determined selectively with the proposed electroanalytical method in the presence of these possible investigated interferents.

The performance of the herein described new inkjet-printed sensor for the detection of paraquat was applied for its quantification in different complex matrices, such as human blood serum, food, and drinking water. These samples were prepared as described in Section 2.1 and fortified with a paraquat standard solution in order to obtain a solution concentration of 30.0 μmol L^{-1}. The determination of the pesticide was performed by interpolating the obtained current value in the previously obtained analytical curve. The voltammograms obtained for each sample can be seen in Figure S6 in Supplementary Materials. By analyzing the results presented in Table 3, it is possible to see that the recoveries ranged from 97% to 113%. Thus, we can infer that paraquat can be successfully determined in different complex matrices by the herein reported printed sensor since there were no significant matrix interferences.

Table 3. Results obtained in the determination of paraquat in water, orange juice, and biological serum samples using the proposed method using the paper-based silver sensor.

Sample	Added (μmol L^{-1})	Found [1] (μmol L^{-1})	Recovered %
Drinking water	30.0	29 ± 4	97 ± 12
Orange juice	30.0	30 ± 1	103 ± 3
Blood serum	30.0	34 ± 2	113 ± 6

[1] $n = 3$.

4. Conclusions

Here, we prepared, characterized, and applied silver inkjet-printed electrodes on paper for the analytical determination of paraquat. The proposed device is cheap and easy to fabricate, and yet its analytical characteristics are comparable to other more complex sensors reported in the literature.

The combination of inkjet-printing technology with a porous paper substrate allowed the electroactive area to be almost 20 times bigger than the geometric area, which resulted in a higher analytical signal; furthermore, a heterogeneous electron transfer constant that was better than or comparable to the same parameter was obtained using modified screen-printed electrodes.

Furthermore, the ink-jet printing technology adopted provided high precision and resolution with great reproducibility of the printed electrodes.

Thus, the simplicity of the proposed method combined with the reported results suggests its reliability and potential for use in routine analysis. The presented results also show the robustness of the method, which can be applied for a wide range of matrices with sufficient accuracy and precision with the advantages of being cost-effective and environmentally friendly.

References

1. Markets and Market. Available online: https://www.marketsandmarkets.com/Market-Reports/printed-electronics-market-197. html?gclid=Cj190KCQiA199P__BRC190ARIsAEZ196irgSR191SFZmKMO570OrbsHSYjrrqCmd105FyCtX-YJnXp192dGcQm193 xJ198sIaAv191sEALw_wcB (accessed on 15 January 2021).
2. Hayat, A.; Marty, J.L.J.S. Disposable screen printed electrochemical sensors: Tools for environmental monitoring. *Sensors* **2014**, *14*, 10432–10453. [CrossRef] [PubMed]
3. Honeychurch, K.C.; Hart, J.P. Screen-printed electrochemical sensors for monitoring metal pollutants. *TrAC Trends Anal. Chem.* **2003**, *22*, 456–469. [CrossRef]
4. Li, M.; Li, D.-W.; Xiu, G.; Long, Y.-T. Applications of screen-printed electrodes in current environmental analysis. *Curr. Opin. Electrochem.* **2017**, *3*, 137–143. [CrossRef]

5. Thiyagarajan, N.; Chang, J.-L.; Senthilkumar, K.; Zen, J.-M. Disposable electrochemical sensors: A mini review. *Electrochem. Commun.* **2014**, *38*, 86–90. [CrossRef]

6. Hartwig, M.; Zichner, R.; Joseph, Y.J.C. Inkjet-printed wireless chemiresistive sensors—A review. *Chemosensors* **2018**, *6*, 66. [CrossRef]

7. Tortorich, R.P.; Shamkhalichenar, H.; Choi, J.-W.J.A.S. Inkjet-printed and paper-based electrochemical sensors. *Appl. Sci.* **2018**, *8*, 288. [CrossRef]

8. Paschoalino, W.J.; Kogikoski, S.K., Jr.; Barragan, J.T.C.; Giarola, J.F.; Cantelli, L.; Rabelo, T.M.; Pessanha, T.M.; Kubota, L.T. Emerging considerations for the future development of electrochemical paper-based analytical devices. *ChemElectroChem* **2019**, *6*, 10–30. [CrossRef]

9. Lee, V.B.C.; Mohd-Naim, N.F.; Tamiya, E.; Ahmed, M.U. Trends in paper-based electrochemical biosensors: From design to application. *Anal. Sci.* **2018**, *34*, 7–18. [CrossRef]

10. Deroco, P.B.; Giarola, J.D.F.; Wachholz Junior, D.; Lorga, G.A.; Kubota, L.T. Paper-based electrochemical sensing devices. *Compr. Anal. Chem.* **2020**, *89*, 91–137. [CrossRef]

11. Noviana, E.; McCord, C.P.; Clark, K.M.; Jang, I.; Henry, C.S. Electrochemical paper-based devices: Sensing approaches and progress toward practical applications. *Lab a Chip* **2020**, *20*, 9–34. [CrossRef]

12. Gonzalez-Macia, L.; Morrin, A.; Smyth, M.R.; Killard, A.J. Advanced printing and deposition methodologies for the fabrication of biosensors and biodevices. *Analist* **2010**, *135*, 845–867. [CrossRef] [PubMed]

13. Li, J.; Rossignol, F.; Macdonald, J. Inkjet printing for biosensor fabrication: Combining chemistry and technology for advanced manufacturing. *Lab a Chip* **2015**, *15*, 2538–2558. [CrossRef] [PubMed]

14. Liana, D.D.; Raguse, B.; Gooding, J.J.; Chow, E. Recent advances in paper-based sensors. *Sensors* **2012**, *12*, 11505–11526. [CrossRef]

15. Singh, A.T.; Lantigua, D.; Meka, A.; Taing, S.; Pandher, M.; Camci-Unal, G. Paper-based sensors: Emerging themes and applications. *Sensors* **2018**, *18*, 2838. [CrossRef] [PubMed]

16. Setti, L.; Fraleoni-Morgera, A.; Ballarin, B.; Filippini, A.; Frascaro, D.; Piana, C. An amperometric glucose biosensor prototype fabricated by thermal inkjet printing. *Biosens. Bioelectron.* **2005**, *20*, 2019–2026. [CrossRef] [PubMed]

17. Moya, A.; Sowade, E.; del Campo, F.J.; Mitra, K.Y.; Ramon, E.; Villa, R.; Baumann, R.R.; Gabriel, G. All-inkjet-printed dissolved oxygen sensors on flexible plastic substrates. *Org. Electron.* **2016**, *39*, 168–176. [CrossRef]

18. Cinti, S.; Arduini, F.; Moscone, D.; Palleschi, G.; Gonzalez-Macia, L.; Killard, A.J. Cholesterol biosensor based on inkjet-printed Prussian blue nanoparticle-modified screen-printed electrodes. *Sens. Actuators B Chem.* **2015**, *221*, 187–190. [CrossRef]

19. Sandström, J.; Broyer, A.; Zoia, D.; Schilt, C.; Greggio, C.; Fournier, M.; Do, K.Q.; Monnet-Tschudi, F. Potential mechanisms of development-dependent adverse effects of the herbicide paraquat in 3D rat brain cell cultures. *NeuroToxicology* **2017**, *60*, 116–124. [CrossRef]

20. Wesseling, C.; Joode, B.V.W.D.; Ruepert, C.; León, C.; Monge, P.; Hermosillo, H.; Partanen, L.J. Paraquat in developing countries. *Int. J. Occup. Environ. Health* **2001**, *7*, 275–286. [CrossRef] [PubMed]

21. Tomková, H.; Sokolová, R.; Opletal, T.; Kučerová, P.; Kučera, L.; Součková, J.; Skopalová, J.; Barták, P. Electrochemical sensor based on phospholipid modified glassy carbon electrode—Determination of paraquat. *J. Electroanal. Chem.* **2018**, *821*, 33–39. [CrossRef]

22. Tcheumi, H.L.; Tassontio, V.N.; Tonle, I.K.; Ngameni, E. Surface functionalization of smectite-type clay by facile polymerization of β-cyclodextrin using citric acid cross linker: Application as sensing material for the electrochemical determination of paraquat. *Appl. Clay Sci.* **2019**, *173*, 97–106. [CrossRef]

23. Pacheco, M.R.; Barbosa, S.C.; Quadrado, R.F.N.; Fajardo, A.R.; Dias, D. Glassy carbon electrode modified with carbon black and cross-linked alginate film: A new voltammetric electrode for paraquat determination. *Anal. Bioanal. Chem.* **2019**, *411*, 3269–3280. [CrossRef]

24. Ghalkhani, M.; Maghsoudi, S.; Saeedi, R.; Khaloo, S.S. Ultrasensitive quantification of paraquat using a newly developed sensor based on silver nanoparticle-decorated carbon nanotubes. *J. Iran. Chem. Soc.* **2019**, *16*, 1301–1309. [CrossRef]

25. Zhang, J.; Lin, Z.; Qin, Y.; Li, Y.; Liu, X.; Li, Q.; Huang, H. Fabricated Electrochemical Sensory Platform Based on the Boron Nitride Ternary Nanocomposite Film Electrode for Paraquat Detection. *ACS Omega* **2019**, *4*, 18398–18404. [CrossRef] [PubMed]

26. Souza, D.C.; Orzari, L.O.; de Oliveira, P.R.; Kalinke, C.; Bonacin, J.A.; Malaspina, O.; Nocelli, R.C.F.; Janegitz, B.C. Electro-chemical sensor based on beeswax and carbon black thin biofilms for determination of paraquat in Apis mellifera Honey. *Food Anal. Methods* **2020**, *14*, 606–615. [CrossRef]

27. Paramalinggam, T.; Yusoff, A.R.M.; Qureshi, M.S.; Shah, Z.A.; Sathishkumar, P.; Yusop, Z.; Khalid, M.; Khokhar, F.M. Determination of paraquat dichloride from water samples using differential pulse cathodic stripping voltammetry. *Russ. J. Electrochem.* **2018**, *54*, 1155–1163. [CrossRef]

28. De Figueiredo-Filho, L.C.; Baccarin, M.; Janegitz, B.C.; Fatibello-Filho, O. A disposable and inexpensive bismuth film minisensor for a voltammetric determination of diquat and paraquat pesticides in natural water samples. *Sens. Actuators B Chem.* **2017**, *240*, 749–756. [CrossRef]

29. Chuntib, P.; Themsirimongkon, S.; Saipanya, S.; Jakmunee, J. Sequential injection differential pulse voltammetric method based on screen printed carbon electrode modified with carbon nanotube/Nafion for sensitive determination of paraquat. *Talanta* **2017**, *170*, 1–8. [CrossRef] [PubMed]

30. Da Silva, E.T.S.G.; Miserere, S.; Kubota, L.T.; Merkoçi, A. Simple on-plastic/paper inkjet-printed solid-state Ag/AgCl pseudoreference electrode. *Anal. Chem.* **2014**, *86*, 10531–10534. [CrossRef]

31. Mocak, J.; Bond, A.M.; Mitchell, S.; Scollary, G. A statistical overview of standard (IUPAC and ACS) and new procedures for determining the limits of detection and quantification: Application to voltammetric and stripping techniques (Technical Report). *Pure Appl. Chem.* **1997**, *69*, 297–328. [CrossRef]

32. Gosser, D.K. *Cyclic Voltammetry: Simulation and Analysis of Reaction Mechanisms*; VCH: New York, NY, USA, 1993; p. 165.

33. Bard, A.J.; Faulkner, L.R. *Electrochemical Methods, Fundamentals and Applications*, 2nd ed.; Wiley: New York, NY, USA, 2001.

34. Csóka, B.; Nagy, G. Determination of diffusion coefficient in gel and in aqueous solutions using scanning electrochemical microscopy. *J. Biochem. Biophys. Methods* **2004**, *61*, 57–67. [CrossRef]

35. Nicholson, R.S. Theory and application of cyclic voltammetry for measurement of electrode reaction kinetics. *Anal. Chem.* **1965**, *37*, 1351–1355. [CrossRef]

36. Lavagnini, I.; Antiochia, R.; Magno, F. An extended method for the practical evaluation of the standard rate constant from cyclic voltammetric data. *Electroanalysis* **2004**, *16*, 505–506. [CrossRef]

37. Foster, C.; Metters, J.P.; Kampouris, D.K.; Banks, C.E. Ultraflexible screen-printed graphitic electroanalytical sensing platforms. *Electroanalysis* **2014**, *26*, 262–274. [CrossRef]

38. Metters, J.P.; Kadara, R.O.; Banks, C.E. Fabrication of co-planar screen printed microband electrodes. *Analist* **2013**, *138*, 2516–2521. [CrossRef]

39. Scremin, J.; Dos Santos, I.V.J.; Hughes, J.P.; Ferrari, A.G.-M.; Valderrama, E.; Zheng, W.; Zhong, X.; Zhao, X.; Sartori, E.J.R.; Crapnell, R.D.; et al. Platinum nanoparticle decorated vertically aligned graphene screen-printed electrodes: Electrochemical characterisation and exploration towards the hydrogen evolution reaction. *Nanoscale* **2020**, *12*, 18214–18224. [CrossRef]

40. De Souza, D.; Machado, S.A.S. Study of the electrochemical behavior and sensitive detection of pesticides using microelectrodes allied to square-wave voltammetry. *Electroanalysis* **2006**, *18*, 862–872. [CrossRef]

41. El Harmoudi, H.; Achak, M.; Farahi, A.; Lahrich, S.; El Gaini, L.; Abdennouri, M.; Bouzidi, A.; Bakasse, M.; El Mhammedi, M. Sensitive determination of paraquat by square wave anodic stripping voltammetry with chitin modified carbon paste electrode. *Talanta* **2013**, *115*, 172–177. [CrossRef]

42. Farahi, A.; Achak, M.; El Gaini, L.; El Mhammedi, M.A.; Bakasse, M. Electrochemical determination of paraquat in citric fruit based on electrodeposition of silver particles onto carbon paste electrode. *J. Food Drug Anal.* **2015**, *23*, 463–471. [CrossRef]

43. Laghrib, F.; Bakasse, M.; Lahrich, S.; El Mhammedi, M. Electrochemical sensors for improved detection of paraquat in food samples: A review. *Mater. Sci. Eng. C* **2020**, *107*, 110349. [CrossRef] [PubMed]

44. Ribeiro, J.A.; Carreira, C.A.; Lee, H.J.; Silva, F.; Martins, A.; Pereira, C.M. Voltammetric determination of paraquat at DNA–gold nanoparticle composite electrodes. *Electrochimica Acta* **2010**, *55*, 7892–7896. [CrossRef]

45. Díaz, T.G.; Cabanillas, A.G.; Salinas, F. Square-Wave and differential pulse oxidative voltammetric determination of diquat and paraquat in alkaline medium. *Electroanalysis* **2000**, *12*, 616–621. [CrossRef]

46. Ye, X.; Gu, Y.; Wang, C. Fabrication of the Cu2O/polyvinyl pyrrolidone-graphene modified glassy carbon-rotating disk electrode and its application for sensitive detection of herbicide paraquat. *Sens. Actuators B Chem.* **2012**, *173*, 530–539. [CrossRef]